universe

MDPI

Review

Measurement of the Hadronic Resonance Production with ALICE at the CERN LHC †

Maria Vasileiou and on behalf of the ALICE Collaboration

Faculty of Physics, National and Kapodistrian University of Athens, GR-15784 Athens, Greece; mvasili@phys.uoa.gr; Tel.: +30-698-244-4082

† This paper is based on the talk at the 7th International Conference on New Frontiers in Physics (ICNFP 2018), Crete, Greece, 4–12 July 2018.

Received: 27 November 2018; Accepted: 20 December 2018; Published: 26 December 2018

Abstract: We present a comprehensive study of hadronic resonance production in pp, p-Pb and Pb-Pb collisions at different Large Hadron Collider LHC energies. In particular, the production of hadronic resonances, such as $\varrho(770)^0$, $K^*(892)^0$, $\varphi(1020)$, $\Sigma(1385)^{\pm}$, $\Lambda(1520)$ and $\Xi(1530)^0$ will be discussed in detail. In heavy-ion collisions, hadronic resonances are sensitive to the re-scattering and regeneration processes occurring between chemical freeze-out and kinetic freeze-out due to their short lifetimes. The measurements in pp and p-Pb collisions are used as a reference for heavy-ion collisions and to search for the onset of collective phenomena. We will report on the transverse momentum spectra, integrated yields, mean transverse momenta, particle ratios and nuclear modification factors of hadronic resonances. The results will be compared to those of other experiments, and to theoretical models and Monte Carlo generators.

Keywords: LHC; ALICE; heavy ion collisions; hadronic resonances; suppression; QCD matter

---

1. Introduction

A large ion collider experiment (ALICE) is designed to study the physics of strongly interacting matter under extremely high temperature and energy density conditions to investigate the properties of the quark-gluon plasma. Over the years, ALICE has measured the production of hadronic resonances in pp, p-Pb, Xe-Xe, and Pb-Pb collisions at the LHC. Due to the short lifetimes of the resonances, their daughter particles in the hadronic decay channels can undergo re-scattering and regeneration in the time interval between the chemical and kinetic freeze-out in heavy-ion collisions. Therefore, the study of resonances with different lifetimes provides information for the characterization of the late stages of the fireball evolution. The measurements in pp and p-Pb constitute a reference for heavy-ion collisions and were also used for tuning the quantum chromodynamics QCD inspired event generators. In these proceeding results on resonance production in pp collisions at $\sqrt{s}$ = 7 and 13 TeV, p-Pb at $\sqrt{s_{\rm NN}}$ = 5.02 TeV, Pb-Pb at $\sqrt{s_{\rm NN}}$ = 2.76 and 5.02 TeV and finally Xe-Xe collisions at $\sqrt{s_{\rm NN}}$ = 5.44 TeV, will be presented.

2. ALICE Detector

The ALICE detector consists of a central part for the measurement of hadrons, electrons and photons and a forward muon spectrometer [1]. The central barrel is contained within a solenoid and addresses particle production at mid-rapidity. It contains an inner tracking system (ITS), a time projection chamber (TPC), a time-of-flight detector (TOF), ring imaging cherenkov (HMPID), and transition radiation detectors (TRD). It also contains two electromagnetic calorimeters (PHOS and EMCAL). The ITS and the TPC are the main tracking detectors, while the ITS, TPC, TOF, and HMPID provide information for particle identification over a wide range in momentum. The ALICE forward detectors include two arrays of scintillator counters (V0 detector), which are used for triggering and centrality determination.

3. Results and Discussion

In the following, we will present results on hadronic resonances production in different collision systems and energies. The resonances are re-constructed from an invariant mass analysis of their identified hadronic decay-product candidates.

3.1. pp and p-Pb Collisions

The p_{T}-integrated yields of K*(892)^0 and φ(1020) as a function of the mean charged-particle multiplicity density are shown in Figure 1 for pp and p-Pb collisions at various energies. One can observe that the yields increased with multiplicity. All measurements are consistent with each other and fall on a single line. This implies that resonance production is independent of colliding system or energy, and scales with multiplicity.

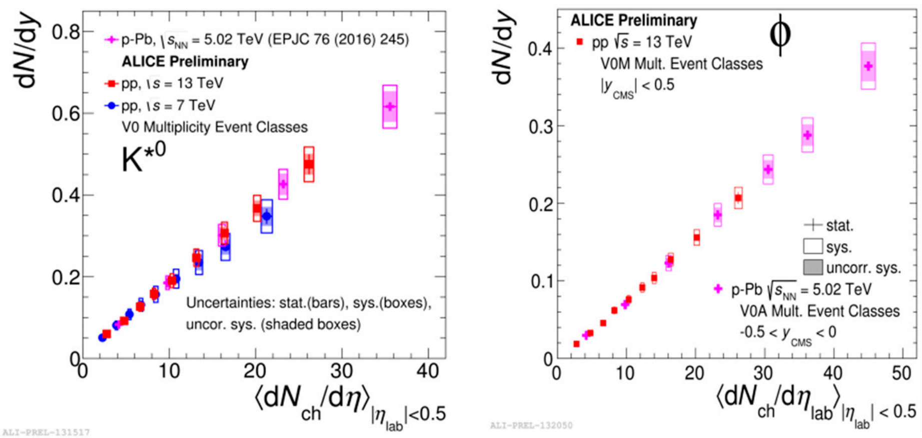

Figure 1. Integrated yield of K*(892)^0 as a function of the mean charged-particle multiplicity density for pp collisions at $\sqrt{s}$ = 7, 13 TeV and p-Pb collisions at $\sqrt{s_{\mathrm{NN}}}$ = 5.02 TeV (**left panel**). Integrated yield of φ(1020) as a function of the mean charged-particle multiplicity density for pp collisions at $\sqrt{s}$ = 13 TeV and p-Pb collisions at $\sqrt{s_{\mathrm{NN}}}$ = 5.02 TeV (**right panel**). Statistical and systematic uncertainties are plotted as vertical error bars and boxes, respectively. The shaded boxes are the multiplicity uncorrelated systematic uncertainties.

Figure 2 represents the integrated yield ratios of excited to ground-state hyperons as a function of the mean charged-particle multiplicity density for different collision systems and energies [2]. The ratios show no multiplicity dependence. Thus, it appears that neither regeneration nor re-scattering affect the resonance yields significantly as a function of multiplicity in these small collision systems. The results were compared with model predictions, PYTHIA8 for pp at 7 TeV and DPMJET for p-Pb at 5.02 TeV collisions. The $\Sigma(1385)^{\pm}$ to Λ ratios were consistent with the values predicted by PYTHIA8 in pp collisions, whereas the DPMJET prediction for p-Pb collisions was lower than the experimental data. The measured $\mathbf{\Xi(1530)^0}$ to Ξ^- ratios appeared higher than the corresponding predictions for both systems. The integrated yield ratios of $\mathbf{\Sigma(1385)}^{\pm}$ and $\Xi(1530)^0$ to pions are presented in Figure 3 as a function of the mean charged-particle multiplicity density for different collision systems and energies. We observed an increasing trend that depended only on the strangeness content. In both cases, QCD-inspired predictions like PYTHIA for pp and DPMJET for p-Pb clearly underestimated the observed yield ratios. The enhancement of higher mass resonances was consistent with the previously reported enhancement of the corresponding lower mass, ground-state particles with the same strangeness content [3].

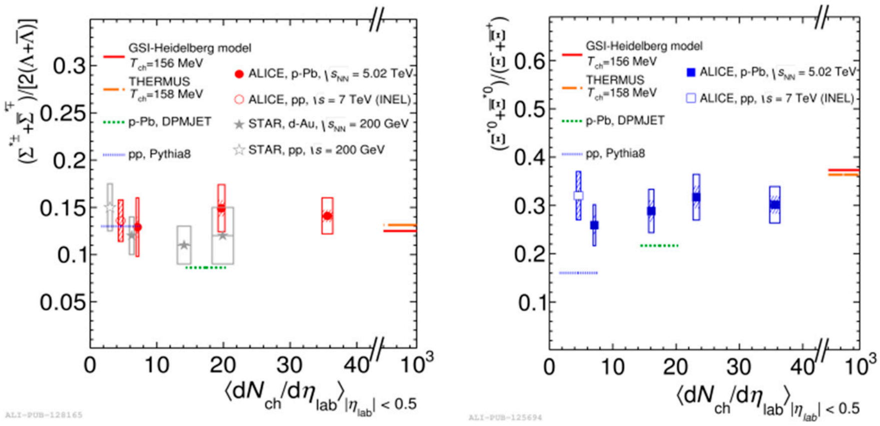

Figure 2. Ratio of $\Sigma(1385)^{\pm}$ to Λ (**left**), $\Xi(1530)^0$ to Ξ^- (**right**) measured in pp, d-Au and p-Pb collisions as a function of the mean charged-particle multiplicity density. Statistical (bars) and systematic uncertainties (boxes) are shown. The shaded boxes are the multiplicity uncorrelated systematic uncertainties. Model predictions are also presented as lines at the appropriate abscissa. Figure taken from [2].

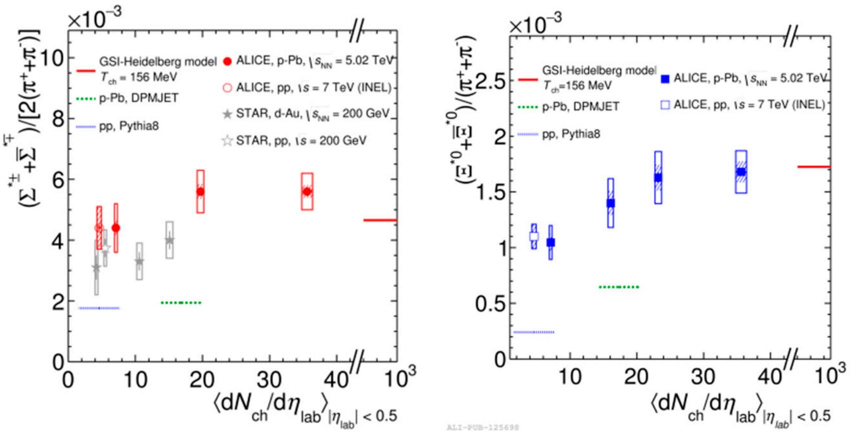

Figure 3. Ratio of $\Sigma(1385)^{\pm}$ to $\pi^{\pm}$ (**left**) and $\Xi(1530)^0$ to $\pi^{\pm}$ (**right**) measured in pp, d-Au and p-Pb collisions as a function of the mean charged-particle multiplicity density. Statistical (bars) and systematic uncertainties (boxes) are shown. The shaded boxes are the multiplicity. Model predictions are also presented as lines at the appropriate abscissa. Figure taken from [2].

3.2. Pb-Pb and Xe-Xe Collisions

The mean transverse momentum values of $\pi^{\pm}$, $K^{\pm}$, $K^*(892)^0$, p and $\varphi(1020)$ are shown in Figure 4 as a function of the mean charged-particle multiplicity density in Pb-Pb collisions at $\sqrt{s_{NN}}$ = 5.02 TeV. All particles exhibited an increase in $<p_T>$ values from peripheral to central Pb-Pb collisions. In central collisions, the mean transverse momentum of $K^*(892)^0$, p and $\varphi(1020)$ were found to be consistent with each other, as expected if the spectral shape is dominated by radial flow. The ratios of the p_T-integrated particle yields $K^*(892)^0/K$ and $\varphi(1020)/K$ are shown in Figure 5 as a function of $<dN_{ch}/d\eta>^{1/3}$, which is a proxy for the system size [4], in pp collisions at $\sqrt{s}$ = 13 TeV, p-Pb collisions at $\sqrt{s_{NN}}$ = 5.02 TeV, Pb-Pb collisions at $\sqrt{s_{NN}}$ = 2.76 and 5.02 TeV and Xe-Xe collisions at $\sqrt{s_{NN}}$ = 5.44 TeV. The ratio $K^*(892)^0/K$ shows a clear suppression going from p-Pb and peripheral Pb-Pb to central Pb-Pb collisions, which is consistent with the re-scattering of the daughters [5]. The ratio $\varphi(1020)/K$ showed an almost constant behavior for all colliding systems, which suggests that re-scattering of the daughters is not significant for $\varphi(1020)$. This is to be expected because the mean lifetime of the $\varphi(1020)$ is about ten times longer than the $K^*(892)^0$. We observed that the measured ratios are consistent between Pb-Pb and Xe-Xe collisions and showed very weak energy dependence in heavy ion collisions (consistent with STAR at RHIC [5,6]).

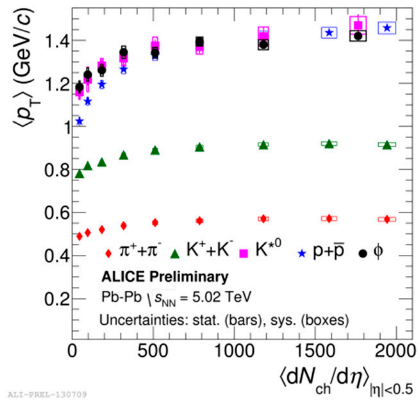

Figure 4. Mean transverse momentum of K*(892)^0 and φ(1020) compared to that identified as $\pi^{\pm}$, $K^{\pm}$ and p as a function of the mean charged-particle multiplicity density in Pb-Pb collisions at $\sqrt{s_{NN}}$ = 5.02 TeV. Statistical uncertainties are represented as bars, whereas boxes indicate systematic uncertainties.

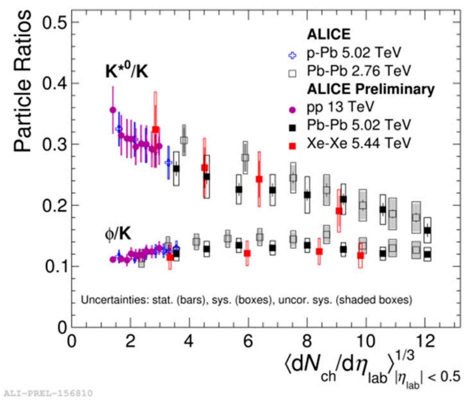

Figure 5. Ratios of p_T-integrated particle yields K*(892)^0/K and φ(1020)/K as a function of $<dN_{ch}/d\eta>^{1/3}$ for different collision systems and energies. The statistical uncertainties are shown as bars. Boxes show systematic uncertainties. The shaded boxes are the multiplicity uncorrelated systematic uncertainties.

The production of the $\varrho(770)^0$ meson were measured at mid-rapidity ($|y| < 0.5$) in pp and centrality differential Pb–Pb collisions at $\sqrt{s_{NN}}$ = 2.76 TeV with the ALICE detector. The particles were reconstructed in the $\varrho(770)^0 \rightarrow \pi^+\pi^-$ decay channel in the transverse momentum (p_T) range 0.5−11 GeV/c. The ratio $\varrho(770)^0/\pi$ as a function of $<dN_{ch}/d\eta>^{1/3}$ in pp and Pb-Pb collisions at $\sqrt{s_{NN}}$ = 2.76 TeV [7] is shown in Figure 6. The ratio shows a significant suppression going from pp, and peripheral Pb-Pb to central Pb-Pb collisions. This behavior is consistent with the re-scattering of the daughter particles in the dense hadron gas. It was observed that EPOS3 with UrQMD [8] qualitatively reproduced the trend of the suppression, while the thermal model [9] overestimates the ratio.

The nuclear modification factor, R_{AA}, is defined as the ratio of the particle yield in Pb-Pb collisions to that in pp scaled by the number of nucleon-nucleon collisions. In absence of nuclear effects R_{AA} was expected to be equal to one. Figure 7 shows the nuclear modification factors as a function of p_T for K*(892)^0 and φ(1020) in Pb-Pb collisions at $\sqrt{s_{NN}}$ = 2.76 TeV for different centrality classes [10]. The results were compared with the R_{AA} of charged hadrons measured by ALICE [11]. The nuclear modification factors of K*(892)^0 and φ(1020) showed similar behavior at high p_T as those of charged hadrons in all centralities. A strong suppression was observed for the most central collisions.

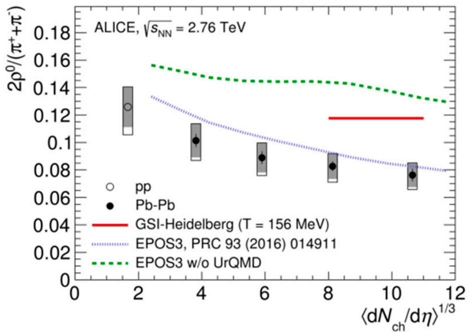

Figure 6. $\varrho(770)^0/\pi$ ratio as a function of <dN_{ch}/dη>$^{1/3}$ in pp and Pb-Pb collisions at $\sqrt{s_{NN}}$ = 2.76 TeV. The statistical uncertainties are shown as bars. Boxes show systematic uncertainties. The shaded boxes are the multiplicity uncorrelated systematic uncertainties. The widths of the boxes are fixed to arbitrary values for better visibility. Figure taken from [7].

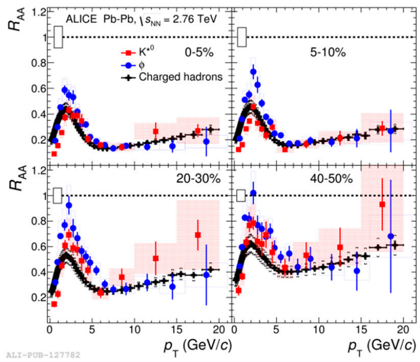

Figure 7. The R_{AA} of K*(892)^0 and φ(1020) as a function of p_T in the 0–5%, 5–10%, 20–30% and 40–50% centrality classes for Pb-Pb collisions at $\sqrt{s_{NN}}$ = 2.76 TeV. The statistical (systematic) uncertainties are shown as bars (boxes). Figure taken from [10].

Figure 8 shows the R_{AA} of K*(892)^0 and φ(1020) as a function of p_T in the most central Pb-Pb collisions at $\sqrt{s_{NN}}$ = 2.76 TeV [10]. The results were compared with the R_{AA} of π, K and p [12]. The nuclear modification factors of the resonances were similar with those of light-flavored hadrons at $p_T > 8$ GeV/c and are equally suppressed by a factor 4–5.

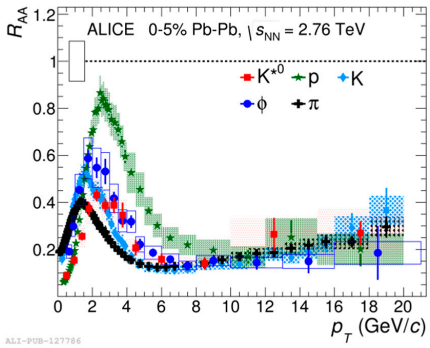

Figure 8. The R_{AA} of K*(892)^0 and φ(1020) as a function of p_T in the 0–5% Pb-Pb collisions at $\sqrt{s_{NN}}$ = 2.76 TeV. The statistical and systematic uncertainties are shown as bars and boxes, respectively. Figure taken from [10].

4. Conclusions

ALICE was used to measure the production of hadronic resonances in pp, p-Pb, Xe-Xe and Pb-Pb collisions. In pp and p-Pb collisions the resonance production seems to be independent of the colliding system or energy and driven only by multiplicity. In central Pb-Pb collisions the mean p_T values of K*(892)^0, p and $\varphi(1020)$ were consistent with each other, as expected if the spectral shape is dominated by radial flow. From the p_T-integrated ratios of the yields of resonances to long lived particles, we found evidence for the re-scattering of the daughters of short-lived resonances in heavy-ion collisions. Strangeness enhancement has been studied with resonances. In small systems the strangeness enhancement as function of multiplicity was found to dependent upon strangeness content rather than particle mass. A strong suppression of high p_T resonances was observed in central Pb-Pb collisions. This demonstrates that resonance production is also affected by strong parton energy loss in the hot and dense QCD medium.

Funding: This research received no external funding.

Conflicts of Interest: The authors declare no conflict of interest.

References

1. ALICE Collaboration. The ALICE experiment at the CERN LHC. *J. Instrum.* **2008**, *3*, S08002.
2. ALICE Collaboration. Production of $\Sigma(1385)^{\pm}$ and $\Xi(1530)^0$ in p-Pb collisions at $\sqrt{s_{\mathrm{NN}}}$ = 5.02 TeV. *Eur. Phys. J. C* **2017**, *77*, 389–403. [PubMed]
3. ALICE Collaboration. Enhanced production of multi-strange hadrons in high-multiplicity proton-proton collisions. *Nat. Phys.* **2017**, *13*, 535–539. [CrossRef]
4. ALICE Collaboration. Two pion Bose-Einstein correlations in central Pb-Pb collisions at $\sqrt{s_{\mathrm{NN}}}$ = 2.76 TeV. *Phys. Lett. B* **2011**, *696*, 328–337. [CrossRef]
5. ALICE Collaboration. K*(892)^0 resonance production in Au+Au and p+p collisions at $\sqrt{s_{\mathrm{NN}}}$ = 200 GeV at STAR. *Phys. Rev. C* **2005**, *71*, 064902–064918. [CrossRef]
6. ALICE Collaboration. Measurements of $\varphi(1020)$ meson production in relativistic heavy-ion collisions at RHIC. *Phys. Rev. C* **2009**, *79*, 064903–064925. [CrossRef]
7. ALICE Collaboration. Production of $\varrho(770)^0$ meson in pp and Pb-Pb collisions at $\sqrt{s_{\mathrm{NN}}}$ = 2.76 TeV. *arXiv*, **2018**; arXiv:1805.04365.
8. Knospe, A.G.; Markert, C.; Werner, K.; Steinheimer, J.; Bleicher, M. Hadronic resonance production and interaction in partonic and hadronic matter in the EPOS3 model with and without the hadronic afterburner UrQMD. *Phys. Rev. C* **2016**, *93*, 014911–014923. [CrossRef]
9. Andronic, A.; Braun-Munzinger, P.; Stachel, J. Thermal hadron production in relativistic nuclear collisions: The hadron mass spectrum, the horn and the QCD phase transition. *Phys. Lett. B* **2009**, *673*, 142–145. [CrossRef]
10. ALICE Collaboration. K*(892)^0 and $\varphi(1020)$ meson production at high transverse momentum in *pp* and Pb-Pb collisions at $\sqrt{s_{\mathrm{NN}}}$ = 2.76 TeV. *Phys. Rev. C* **2017**, *95*, 064606–064621. [CrossRef]
11. ALICE Collaboration. Centrality dependence of charged particle production at large transverse momentum in Pb-Pb collisions at $\sqrt{s_{\mathrm{NN}}}$ = 2.76 TeV. *Phys. Lett. B* **2013**, *720*, 52–62. [CrossRef]
12. ALICE Collaboration. Production of charged pions, kaons and protons at large transverse momenta in pp and Pb-Pb collisions at $\sqrt{s_{\mathrm{NN}}}$ = 2.76 TeV. *Phys. Lett. B* **2014**, *736*, 196–207.